

THREE-DIMENSIONAL STRESS DISTRIBUTION OF A RIGID WHEEL ON LUNAR REGOLITH SIMULANT

*Shoya Higa¹, Kazumasa Sawada², Keigo Teruya³, Kenji Nagaoka⁴, Kazuya Yoshida⁵

¹ Tohoku University, Aoba 6-6-01, Aramaki, Aoba-ku, Sendai, Japan, E-mail: shoya@astro.mech.tohoku.ac.jp

² Tohoku University, Aoba 6-6-01, Aramaki, Aoba-ku, Sendai, Japan, E-mail: sawada@astro.mech.tohoku.ac.jp

³ Tohoku University, Aoba 6-6-01, Aramaki, Aoba-ku, Sendai, Japan, E-mail: teruya@astro.mech.tohoku.ac.jp

⁴ Tohoku University, Aoba 6-6-01, Aramaki, Aoba-ku, Sendai, Japan, E-mail: nagaoka@astro.mech.tohoku.ac.jp

⁵ Tohoku University, Aoba 6-6-01, Aramaki, Aoba-ku, Sendai, Japan, E-mail: yoshida@astro.mech.tohoku.ac.jp

ABSTRACT

For estimation and control of the wheeled mobility of a lunar/planetary exploration rover, three-dimensional stress distribution measurements and a theoretical model of a rigid wheel on loose soil is quite important. We developed a single wheel testbed for use in comprehensive experiments, to understand the wheel-soil interaction, and measured the normal, circumferential, and lateral stress distributions beneath the wheel on lunar regolith simulant. These experiments yielded estimates of the shear stress direction and the soil flow directions, by combining the two-directional shear stress distributions. We validated the measurements by integrating the vertical components of the normal and shear stress distributions. The classical shear stress model was also compared with the measurements. We found no significant difference between the model and the measurements performed on lunar regolith simulant under three different slip conditions.

1 INTRODUCTION

Most lunar/planetary exploration rovers employ wheel-based locomotion because of its mechanical simplicity, reliability, controllability, and efficiency. However, wheels easily slip on surfaces covered with fine granular regolith, as found on the moon or Mars. Wheel slippage hinders robotic operations such as localization or motion along a path. Furthermore, the risk of a rover getting stuck is a critical problem in lunar/planetary exploration missions. In fact, one of the twin Mars Exploration Rovers, named Spirit, of the National Aeronautics and Space Administration (NASA), has been unable to continue planned mission since its wheel got stuck in the loose Martian regolith, as it attempted to traverse a hilly region [1]. Future rovers therefore require mechanisms that will prevent such problems in loose soil.

To avoid a sand trap, it is necessary to understand the process of wheel slippage itself. Generally, the trap occurs in situations that favor the digging of wheel into the ground and slippage. These phenomena interact at

the mechanical interface between the traveling wheel and the soil. From a perspective of terramechanics (research field concerned with terrain-vehicle systems), loose soil received much attention [2, 3]. The forces acting on a wheel (e.g., the normal force and the drawbar pull) have been modeled using the normal and shear stress distributions at the contact patch. The stress distributions on the wheel surface have been measured and modeled semi-empirically [4, 5, 6, 7, 8]. Classical models in terramechanics consider mainly heavy vehicles with large wheels and do not therefore apply to small exploration rovers [9]. Thus, new model of the stress distributions relevant to rovers is needed to estimate their performance precisely.

Several researchers have also studied the stress distributions beneath a wheel of lightweight vehicles [10, 11, 12, 13]. We developed an in-wheel measurement device that can measure two-dimensional stress distributions along both the circumferential and axial direction [14]. Although the developed device cannot detect the shear stress distribution, its measurement is essential for understanding the underlying physics of the wheel. We therefore improved the device to detect the shear stress distribution on the wheel surface [15].

On the other hand, the stress distributions of a wheel depend strongly on the soil characteristics. A precise estimate of the mobility performance in loose soil requires experiments done on soil that can appropriately simulate the physical and mechanical characteristics of the terrain of interest. In consideration of future lunar exploration missions, several researchers therefore conducted experiments to clarify the slip characteristics when traveling on a lunar regolith simulant [16, 17, 18]. However, the associated stress distributions were not discussed. In this study, we therefore measured the three-dimensional stress distributions beneath a wheel traveling on lunar regolith simulant.

This paper first describes the experimental setup of our comprehensive single wheel testbed. We then discuss the measured stress distributions beneath the wheel traveling on lunar regolith simulant under various slip conditions. We also validate the measurements by comparing

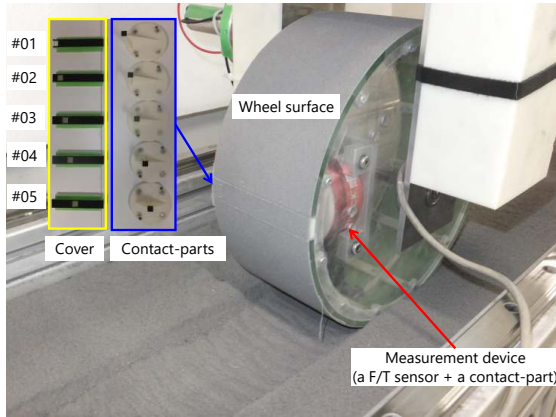


Figure 1: Measurement device inside a wheel.

the actual and estimated wheel loads.

2 EXPERIMENTAL SETUP

To measure the three-dimensional stress distribution on a rigid wheel surface, we developed a single wheel testbed containing a fixed sensing system. We first describe this measurement device and then the single wheel testbed.

2.1 Measurement Device

The measurement device used in this study, shown in Figure 1, consists of a six-axis force and torque (F/T) sensor and five types of “contact-parts.” The F/T sensor detects the three-axial force and three-axial torque data independently. The five types of contact-parts are designed to contact with ten specific measurement points on the wheel surface. The sensing area of each contact-part is 10 mmf × 10 mm. Each contact-part exposed to the wheel surface yields a measurement. Contact was made at locations ±0–10 mm, ±10–20 mm, ±20–30 mm, ±30–40 mm, and ±40–50 mm from the wheel center. We fixed a contact-part on the F/T sensor, and installed this component inside the wheel (the same wheel that was used in a previous study [15]). The areas of the wheel that were not exposed to the contact-parts were covered with the same material as on the wheel surface.

Sand cloth was also pasted onto the wheel surface and to the contact-part exposed to the wheel surface. The sand cloth roughness is nearly same as the average grain diameter of Toyoura standard sand [19]. The particle diameter distribution of lunar regolith simulant (FJS-1 [20]) is wider than Toyoura standard sand and its range of the grain diameters of is smaller than Toyoura standard sand. Lunar regolith simulant adhered to the sand cloth that was pasted to the wheel surface throughout the experiments. Friction on the wheel surface was therefore regarded to be equal to or greater than lunar regolith simulant. Hence, we consider that there is no slippage of the wheel surface

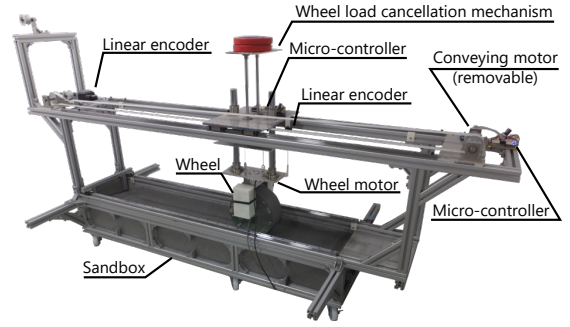


Figure 2: Overview of the single wheel testbed.

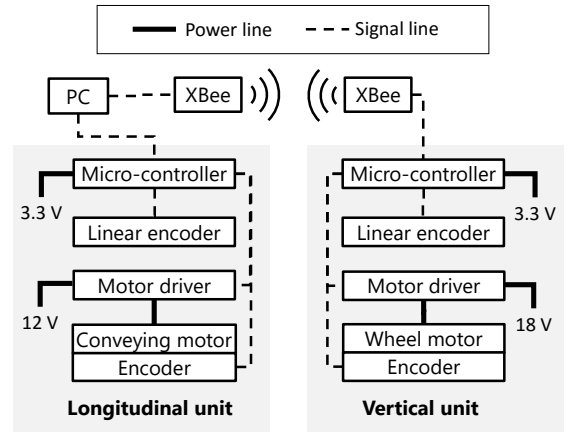


Figure 3: System diagram of the single wheel testbed

throughout traveling experiment. We calibrated the sensor output using a balance weight and pulley before performing the stress measurements.

2.2 Single Wheel Testbed

To conduct an effective and comprehensive experiment on the wheel-soil interaction, we developed the single wheel testbed, shown in Figure 2. The testbed, which includes the sandbox, is 2.50 m long, 1.05 m wide, and 1.25 m high. Figure 3 outlines the single wheel testbed system, consisting of a vertical unit, longitudinal unit, and a sandbox. This section describes the system in detail.

2.2.1 Vertical Unit

The vertical unit consists of two vertical slide shafts and bushes, a wheel that is controlled by a given rotational speed profile, a wheel load cancellation mechanism, and a linear encoder for doing the wheel sinkage measurement. The wheel can move freely in the vertical direction via the vertical slide guide.

A micro-controller maintains a constant rotational velocity via a motor driver under PI control at 10 ms intervals, and measures the wheel sinkage by counting the linear encoder signals at the same intervals. The linear-encoder resolution for the wheel sinkage measurement was 25 μm. Measurements were calibrated by assigning

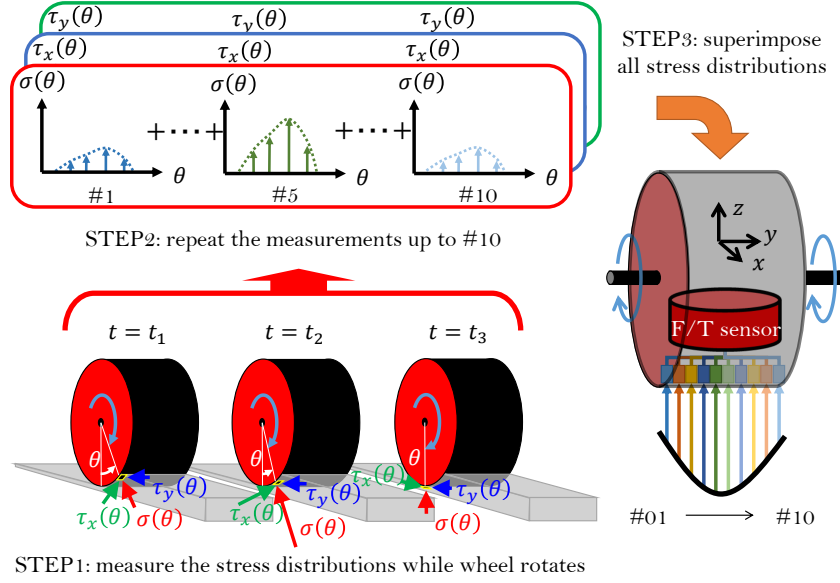


Figure 4: Measurement process of three-dimensional stress distribution on the wheel surface.

the zero level to the soil surface.

2.2.2 Longitudinal Unit

The longitudinal unit consists of two longitudinal linear guides, a conveying motor, and a linear encoder for use in the wheel traveling distance measurement. The conveying motor and timing pulley were coupled, and the timing pulley tightly connected to the vertical unit via a timing belt. The mode of experiments (forced or free slip experiment mode using several traction loads) can be selected by connecting additional rope to the timing belt.

The linear encoder for the wheel traveling distance measurement was connected to the vertical unit. The conveying motor was also PI-controlled using a micro-controller via a motor driver at 10 ms intervals. The micro-controller also counted the wheel traveling distance by the same intervals. The resolution of the linear encoder for the wheel traveling distance was $50 \mu\text{m}$.

2.2.3 Sandbox

The testbed was mounted onto a sandbox of length 1.6 m, width 0.3 m, and depth 0.2 m. Two such sandboxes can be selected to perform experiments on two types of soil. One sandbox is filled with Toyoura standard sand, and the other with lunar regolith simulant (FJS-1).

We mounted the testbed onto the sandbox filled with the lunar regolith simulant, and measured the three-dimensional stress distribution on the wheel surface. The lunar regolith simulant provides a good approximation to the soil characteristics at the moon surface.

2.3 Measurement Method

As shown in Figure 4, the normal stress distribution and two orthogonal shear stress distributions were measured

for each slip ratio s using the following procedure:

- (1) Set #1 contact-part onto the F/T sensor and fix a measurement device into the wheel.
- (2) Mix and rake the soil in the sandbox to form a flat surface.
- (3) Measure the normal, circumferential, and lateral stress distributions with each angle of the wheel rotation.
- (4) Repeat step (2) and (3) three times, and average three measurements under the same conditions.
- (5) Replace the contact-part at each measurement point, and repeat step (2)–(4) up to the point #10.
- (6) Obtain the entire three-dimensional stress distribution of the wheel by superimposing the three-dimensional stress distributions at all ten points on the wheel surface.

The slip ratio s is a key experimental parameter defined as

$$s = 1 - \frac{v_x}{r\omega}, \quad (0 \leq s \leq 1), \quad (1)$$

where r is the wheel radius, ω the wheel angular velocity, and v_x the wheel traveling speed.

3 MEASUREMENT OF THREE-DIMENSIONAL STRESS DISTRIBUTION ON A RIGID WHEEL

This section describes the measurement of the three-dimensional (normal, circumferential, and lateral) stress distribution on a rigid wheel surface.

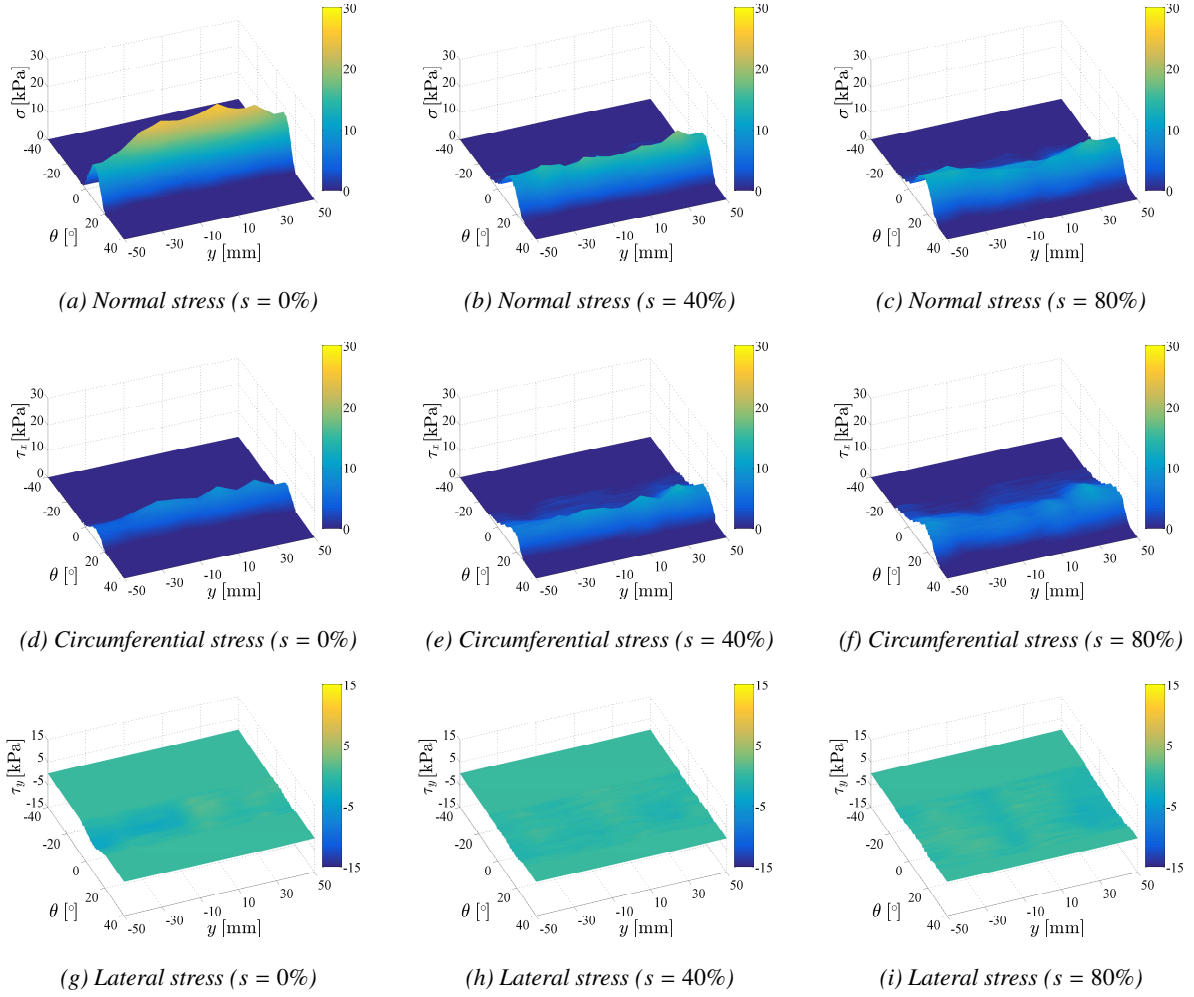


Figure 5: Measurement results of three-dimensional stress distribution on rigid wheel surface.

3.1 Experimental Condition

We measured the three-dimensional stress distribution on lunar regolith simulant for three types of slip ratio.

- The wheel diameter and its width were 250 mm and 100 mm.
- The wheel circumferential velocity was controlled to remain at 2 cm/s throughout the experiment.
- Three types of slip ratios (0%, 40%, and 80%) were input.
- The wheel load was set to 50 N using a wheel load cancellation mechanism.
- The terrain condition was flat.

3.2 Measurement Results and Discussion

In this study, we measured the normal, circumferential, and lateral stress distributions at contact patch on lunar

regolith simulant. The three-dimensional stress distributions were measured at each angle of the wheel rotation. The sensing domain of the contact-parts was exposed to a specific point on the wheel surface at a time. The experiments were carried out under three types of forced slip conditions.

Figure 5 shows the measurement results under three slip conditions. The x -axis in each graph corresponds to the wheel rotation angle θ , the y -axis to the positions y in the wheel axial direction, and the z -axis and color bar to the stress values.

Each stress distribution is generated mainly in the front portion of the wheel. The normal stress distribution decreases and the circumferential stress distribution increases with increasing the slip ratio.

The normal stress distribution in the axial direction, when traveling on the lunar regolith simulant under 0% slip condition, showed that the stress generated near the wheel center is greater than near the edge because the soil near the edge is pushed toward the lateral side of the

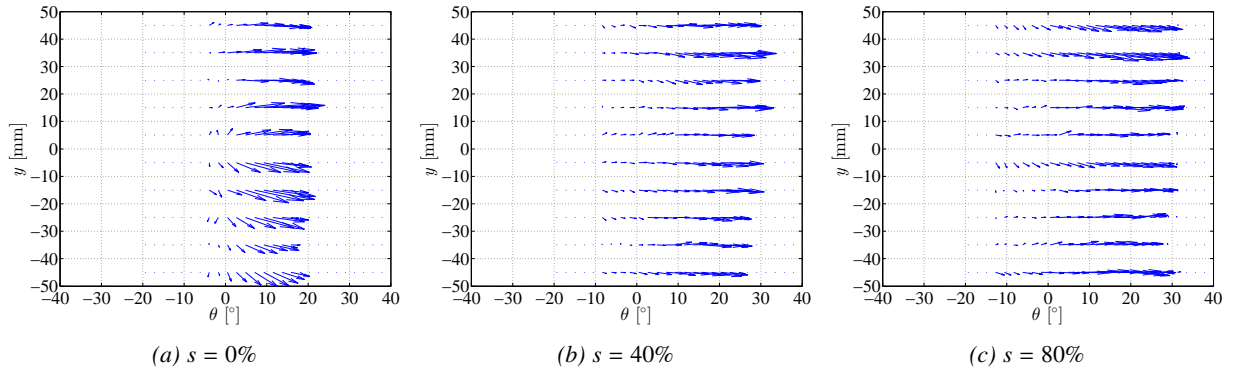


Figure 6: Generating directions of the shear stress on the wheel surface.

wheel. However, the distributions in the axial direction under the other slip conditions are almost flat.

Under the conditions used in this study, the lateral stress distributions were smaller than the other stress distributions, because the wheel has no steering angle. Whereas the soil cohesion differs, the distribution for Toyoura standard sand showed similar trend [14, 15].

Figure 6 shows the generating directions of the shear stresses, which were combined two-axial shear stresses (circumferential and lateral stresses). The horizontal axis represents the wheel rotation angle θ , and the vertical axis the measurement position in the axial direction. The arrows indicate the shear stress directions on the wheel surface.

The generating directions of the shear stress are related because it is induced by the soil movement beneath the traveling wheel. The results suggest that most of the soil moves against the direction of the wheel rotation. In other words, the soil is propelled forward by the traveling wheel. Moreover, the shear stress magnitude is reduced and almost vanishes as the wheel rotation angle approaches the zero position. In other words, the soil motion switches direction and the soil is mostly removed from the wheel surface.

On the other hand, the soil is pushed to lateral side of the wheel under the 0% slip condition. This only occurs under low slip condition, because almost all of the soil beneath the wheel is conveyed backward by the wheel rotation under other slip conditions.

4 EVALUATION OF THE MEASUREMENT RESULTS

To evaluate the measured stress distribution, we integrated the vertical components of the normal and circumferential stress distributions and compared this result with the wheel load. We also evaluated the classical shear stress model by comparing the measured circumferential stress distribution with the model-based shear stress distribution.

4.1 Calculation of the Normal Force of the Wheel

The normal force acting on the wheel can be calculated by integrating the vertical components of the normal stress $\sigma(\theta)$ and the circumferential stress $\tau_x(\theta)$ at all contact patch with the lunar regolith simulant. The normal force F_z is calculated as

$$F_z = r \int_{-b/2}^{b/2} \int_{\theta_r}^{\theta_f} \{\tau_x(\theta) \sin \theta + \sigma(\theta) \cos \theta\} d\theta dy, \quad (2)$$

where b is the wheel width and θ_f and θ_r are the entry and the exit angles into and out of the soil, respectively. The wheel rotation angle θ is zero below the wheel and increases in the counterclockwise direction. We measured the circumferential stress distribution at ten points, and therefore the vertical components at these points were also integrated in the axial direction. This calculation neglects the lateral stress distribution $\tau_y(\theta)$.

4.2 Shear Stress Model

Janosi and Hanamoto proposed a shear stress model based on the direct shear test results [22]. From their model, we can calculate the shear stress at the contact patch using the normal stress and several soil parameters as follows:

$$\tau(\theta) = (c + \sigma(\theta) \tan \phi) [1 - e^{-j_x(\theta)/k_x}], \quad (3)$$

Table 1: Calculation parameters for Lunar regolith simulant (FJS-1)

Parameter	Value	Unit	Source
c	8	[kPa]	[20]
ϕ	37.2	[°]	[20]
k_x	0.02	[m]	[21]
θ_f	20	[°]	Experiment ($s = 0\%$)
θ_r	-6	[°]	Experiment ($s = 0\%$)
θ_f	28	[°]	Experiment ($s = 40\%$)
θ_r	-10	[°]	Experiment ($s = 40\%$)
θ_f	32	[°]	Experiment ($s = 80\%$)
θ_r	-15	[°]	Experiment ($s = 80\%$)

Table 2: Actual wheel load vs. estimated wheel load on lunar regolith simulant.

Slip ratio [%]	Actual wheel load [N]	Estimated wheel load [N]		Error [%]	
		(I) ^a	(II) ^b	(I) ^a	(II) ^b
0	50	55.3	52.9	10.6	5.8
40	50	50.2	51.9	0.5	3.8
80	50	53.4	54.7	6.8	9.4

^a The values of (I) are calculated from all of the measured data.

^b The values of (II) are calculated from the measured normal and shear stress distributions calculated with Equation 4.

where c is the soil cohesion, ϕ an internal friction angle of the soil, k_x a soil deformation modulus, and $j_x(\theta)$ the shear displacement at the wheel rotation angle θ calculated as

$$j_x(\theta) = r[\theta_f - \theta - (1 - s)(\sin \theta_f - \sin \theta)]. \quad (4)$$

4.3 Estimation Error of the Wheel Load from the Stress Distributions

The relative error of the estimation result, E_{est} , between the actual wheel load W_{act} and the estimated wheel load W_{est} is defined as

$$E_{est} = \left(\frac{W_{est}}{W_{act}} - 1 \right) \times 100. \quad (5)$$

The equations mentioned above were calculated using the parameters listed in Table 1.

4.4 Evaluation Results

This study compared the actual wheel load with an estimated wheel load, calculated using the measurement results. The initial rise and fall of the each stress distribution were taken as marking the entry and exit angles, respectively.

Table 2 shows the relative errors between the estimated weights under each condition. All estimations were greater than the actual wheel load, but all errors were less than 11%. This signifies that the shear stress can be estimated reliably, provided the normal stress distribution and the soil parameters are known. There is therefore no significant difference between the model-based and measured shear stress.

Previously, we performed three-dimensional stress measurements using Toyoura standard sand, and confirmed similar trends. We therefore conclude that our measurement method is effective for any type of dry sand.

5 CONCLUSION

This study examined the three-dimensional stress distribution on a rigid wheel traveling on lunar regolith simulant. We first described the single wheel testbed that was used for conducting comprehensive experiments. We then performed three-dimensional stress measurements on a wheel using lunar regolith simulant.

The measurements showed almost same trends as the results in previous works using Toyoura standard sand. The evaluation results indicated that there is no significant difference between the model-based and measured shear stresses.

Future work will consider additional experiments with different slip conditions to model the stress distribution.

References

- [1] R. A. Kerr. Planetary science. mars rover trapped in sand, but what can end a mission? *Science (New York, N.Y.)*, 324(5930):998, May 2009.
- [2] M. G. Bekker. *Theory of Land Locomotion*. University of Michigan Press, Ann Arbor, MI, 1956.
- [3] J. Y. Wong. *Theory of Ground Vehicles*. John Wiley & Sons, Inc., Hoboken, New Jersey, fourth edition, 2008.
- [4] O. Onafeko and A.R. Reece. Soil stresses and deformations beneath rigid wheels. *Journal of Terramechanics*, 4(1):59–80, January 1967.
- [5] J. Y. Wong. Behaviour of soil beneath rigid wheels. *Journal of Agricultural Engineering Research*, 12(4):257 – 269, 1967.
- [6] G. Krick. Radial and shear stress distribution beneath rigid wheels and pneumatic tyres on yielding soils with regard to tyre deformation. *Journal of Terramechanics*, 6(3):73 – 98, 1969.
- [7] A. Oida, A. Satoh, H. Itoh, and K. Triratanasirichai. Three-dimensional stress distributions on a tire-sand contact surface. *Journal of terramechanics*, 28(4):319–330, 1991.
- [8] S. Wanjii, T. Hiroma, Y. Ota, and T. Kataoka. Prediction of wheel performance by analysis of normal and tangential stress distributions under the wheel-soil interface. *Journal of Terramechanics*, 34(3):165–186, may 1997.
- [9] M. G. Bekker. *Introduction to terrain-vehicle systems*. University of Michigan Press, Ann Arbor, MI, 1969.
- [10] K. Nagatani, A. Ikeda, K. Sato, and K. Yoshida. Accurate estimation of drawbar pull of wheeled mobile robots traversing sandy terrain using built-in force sensor array wheel. In *Proceedings of the 2009 IEEE/RSJ International Conference on Intelligent Robots and Systems*, pages 2373–2378, St. Louis, MO, USA, Oct. 2009.

- [11] G. Meirion-Griffith and M. Spenko. A modified pressuresinkage model for small, rigid wheels on deformable terrains. *J. Terramechanics*, 48(2):149–155, apr 2011.
- [12] C. Senatore and K. Iagnemma. Analysis of stress distributions under lightweight wheeled vehicles. *Journal of Terramechanics*, 51:1–17, February 2014.
- [13] T. Shirai and G. Ishigami. Development of in-wheel sensor system for accurate measurement of wheel terrain interaction characteristics. *Journal of Terramechanics*, 62:51–61, 2015.
- [14] S. Higa, K. Nagaoka, K. Nagatani, and K. Yoshida. Measurement and modeling for two-dimensional normal stress distribution of wheel on loose soil. *J. Terramechanics*, 62:63–73, dec 2015.
- [15] S. Higa, K. Sawada, K. Nagaoka, K. Nagatani, and K. Yoshida. Three-dimensional stress distribution on a rigid wheel surface for a lightweight vehicle. In *Proceedings of the 13th European Conference of the ISTVS*, pages 383–391, Rome, 2015.
- [16] S. Wakabayashi, H. Sato, and S. Nishida. Design and mobility evaluation of tracked lunar vehicle. *Journal of Terramechanics*, 46(3):105–114, 2009.
- [17] T. Kobayashi, Y. Fujiwara, J. Yamakawa, N. Yasufuku, and K. Omine. Mobility performance of a rigid wheel in low gravity environments. *Journal of Terramechanics*, 47(4):261–274, 2010.
- [18] M. Sutoh, K. Nagaoka, K. Nagatani, and K. Yoshida. Design of wheels with grousers for planetary rovers traveling over loose soil. *Journal of Terramechanics*, 50(5-6):345–353, October 2013.
- [19] Toyoura Keiseki Kogyo Co., Ltd. About toyoura sand. <http://www.toyourakeiseki.com/english/about.html>, visited on 2014/06/17.
- [20] H. Kanamori, S. Udagawa, T. Yoshida, S. Matsumoto, and K. Takagi. Properties of Lunar Soil Simulant Manufactured in Japan. *Space 98 (6th)*, April 26-30, pages 462–468, 1998.
- [21] M. Sutoh. *Traveling Performance Analysis of Lunar/Planetary Robots on Loose Soil*. PhD thesis, Tohoku University, March 2013.
- [22] Z. Janosi and B. Hanamoto. The analytical determination of drawbar pull as a function of slip for tracked vehicles in deformable soils. In *Proceedings of the 1st International Conference on Terrain-Vehicle Systems*, pages 707–736, Turin, Italy, 1961.